DELFT UNIVERSITY OF TECHNOLOGY

REPORT 89-35

A cell-centered multigrid method for three-dimensional anisotropic-diffusion and interface problems

M. Khalil and P. Wesseling

ISSN 0922-5641

Reports of the Faculty of Technical Mathematics and Informatics no. 89-35

Delft 1989

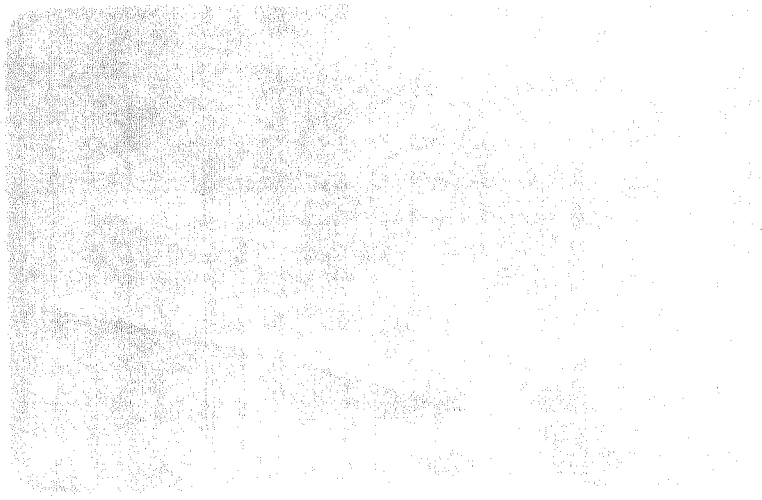

SUMMARY

Three–dimensional interpolatory prolongation and restriction operators for cell–centered multigrid and a new smoother are presented. This smoother is based on a modification of incomplete point factorization. The multigrid method is applied to three–dimensional anisotropic interface problems.

Numerical results show good performance of the method in all cases when accelerated by a Lanczos type method (namely Orthomin). Comparison of storage and computing work required by cell–centered and vertex–centered multigrid methods is given.

1. INTRODUCTION

The aim of this report is to present an extension of the cell–centered multigrid method considered in [14] to three dimensions. We are interested in problems of the following type:

$$-\sum_{\alpha=1}^{3} \frac{\partial}{\partial x_\alpha}\left(D_\alpha \frac{\partial \varphi}{\partial x_\alpha}\right) + \sigma\varphi = f, \quad x \in \Omega = \prod_{\alpha=1}^{3} (0, L_\alpha) \tag{1.1a}$$

with boundary conditions

$$b\frac{\partial \varphi}{\partial n} + c\varphi = g \qquad x \in \partial\Omega \tag{1.1b}$$

with $b \geq 0$, $c \geq 0$, $b + c > 0$, n the normal to the boundary directed away from the interior of Ω.

D_α (>0), σ (≥ 0) and f are given functions allowed to be discontinuous across internal interfaces.

Vertex–centered multigrid methods for such problems using matrix–dependent transfer operators are considered in [1,2,3,4,9,10]. The calculation of the matrix–dependent transfer operators and the related Galerkin approximation of coarse grid matrices are complex and costly. Considerable storage is involved. These two reasons motivated the introduction of the cell–centered multigrid method [14]. It was found in [7] that for two–dimensional interface problems the cell–centered multigrid method is as efficient as the vertex–centered one.

In this report, cell–centered multigrid is extended to three dimensions. Three–dimensional interpolating prolongation and restriction operators related to standard cell–centered coarsening are given. They are chosen such that the coarse grid matrices resulting from Galerkin approximation have optimal sparsity.

Robust smoothing methods are complicated in three dimensions. For general anisotropic cases (D_1, D_2, D_3 widely different) alternating plane relaxation has to be used [5,12]. The powerful incomplete block LU factorization smoother in two dimensions is not completely robust in three dimensions [3,5,8]. Here,, we use the not completely robust but simple point incomplete factorization modified smoother [8]. Numerical results for some test problems with interfaces and

anisotropy are presented. The preliminary work required by cell–centered multigrid is given and compared to that of vertex–centered multigrid.

2. TRANSFER OPERATORS

In this section only two grids need to be considered. Coarse grid quantities are indicated by an overbar. Using cell–centered coarsening, a coarse cell $\bar{\Omega}_i$ is defined to be the union of eight fine cells Ω_{2i+n} intersecting in the center of $\bar{\Omega}_i$, $i \in \mathbb{I}^3$ being the cell center index:

$$\bar{\Omega}_i = \bigcup_n \Omega_{2i+n} \ , \ n \in \{-1,0\}^3. \tag{2.1}$$

This is illustrated by Figure 2.1.

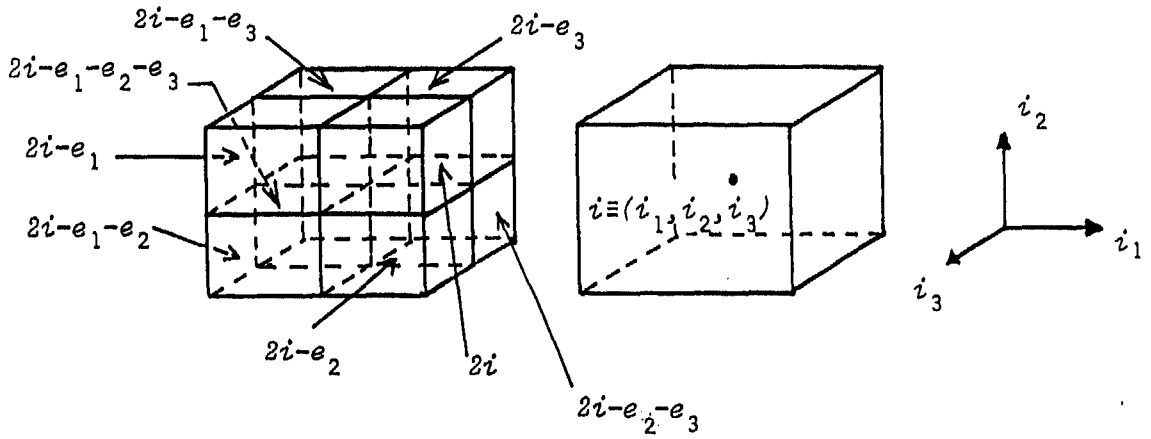

Figure 2.1. Cell–centered coarsening and cell numbering in three dimensions,

$$e_1 = (1,0,0) \ , \ e_2 = (0,1,0) \text{ and } e_3 = (0,0,1).$$

Let the discrete fine grid problem to be solved be denoted by

$$A\varphi = b. \tag{2.2}$$

For ease of exposition we assume that the cells are cubes. Linear interpolation takes place in tetrahedrons, such that linear interpolation results in an R^T, R being the restriction operator, for which the structure of the stencil of $\bar{A}$ is the same as that of A under coarse grid Galerkin approximation:

$$\bar{A} = RAP \tag{2.3}$$

where P is the prolongation.

It was found that a suitable three–dimensional generalization of the two–dimensional structure (the sparsest one permitting discretization of the general elliptic partial differential operator in two dimensions):

$$\begin{bmatrix} * & * & \\ * & * & * \\ & * & * \end{bmatrix}$$

is

$$[A]^{(-1)} = \begin{bmatrix} 0 & 0 & \\ 0 & * & * \\ & * & * \end{bmatrix}, [A]^{(0)} = \begin{bmatrix} * & * & \\ * & * & * \\ & * & * \end{bmatrix}, [A]^{(1)} = \begin{bmatrix} * & * & \\ * & * & 0 \\ & 0 & 0 \end{bmatrix} \tag{2.4}$$

where $[A]^{(\alpha)}$ is the representation of the stencil in the z–constant plane $i_3+\alpha$. Figure 2.2 gives the division of cube in tetrahedrons; capital letters and small letters designate centers of coarse cells and fine cells, respectively

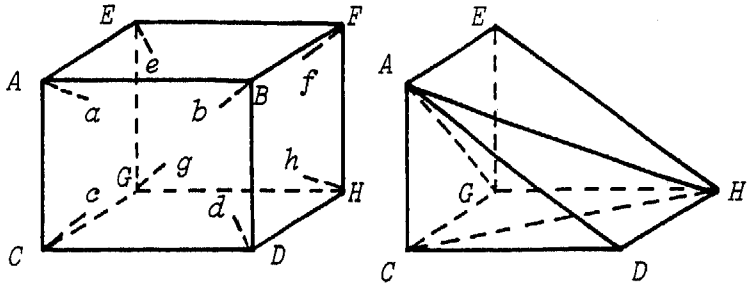

Figure 2.2. Division of cube in tetrahedrons

We found only one partitioning of the cube that results in a restriction operator such that with P given by

$$]P[^{(\alpha)} = \begin{bmatrix} 1 & 1 & \\ & & \\ 1 & 1 & \end{bmatrix}, \quad \alpha = -1,0 \tag{2.5}$$

and $\bar{A}$ by (2.3), the structure of the stencil of $\bar{A}$ is the same as that of A (2.4). Note that P given by (2.5) is a piecewise constant interpolation with $m_p = 1$ (m_p–1 is the maximum degree of polynomials that are interpolated exactly by P). The tetrahedrons are chosen such that those sides that are not parallel to the coordinate axes are either

- parallel to the diagonals in the i_1, i_2, i_3 planes of the stencil of A; these diagonals are the line segments AA, BB, CC in Figure 2.3,

or

- their orthogonal projection on these planes has one of the directions just specified.

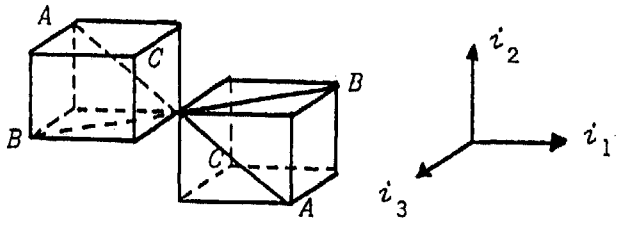

Figure 2.3. Three–dimensional sketch of stencil of A, with diagonals AA, BB, CC.

The tetrahedrons are not to intersect each other. Their union is the cube. In this way the partitioning given in Figure 2.2 is obtained, where we have the following tetrahedrons: ACDH, ACGH, AEGH and by symmetry: HAEF, AEHB, ABHD.

The fine grid points in which function values have to be specified by interpolation are denoted $a,b,\ldots,g,h$ in Figure 2.2. By linear interpolation in the tetrahedrons just specified one obtains:

$$4\phi_a = 3\bar{\phi}_A + \bar{\phi}_H, \quad 4\phi_b = 2\bar{\phi}_B + \bar{\phi}_A + \bar{\phi}_H, \quad 4\phi_c = 2\bar{\phi}_C + \bar{\phi}_A + \bar{\phi}_H,$$
$$4\phi_d = 2\bar{\phi}_D + \bar{\phi}_A + \bar{\phi}_H, \quad 4\phi_e = 2\bar{\phi}_E + \bar{\phi}_A + \bar{\phi}_H, \quad 4\phi_f = 2\bar{\phi}_F + \bar{\phi}_A + \bar{\phi}_H,$$
$$4\phi_g = 2\bar{\phi}_G + \bar{\phi}_A + \bar{\phi}_H, \quad 4\phi_h = \bar{\phi}_A + 3\bar{\phi}_H. \tag{2.6}$$

The boundary modifications are obtained as follows. If A is the center of a coarse boundary cell, such that H lies outside the domain, ϕ_a is obtained by interpolation between A and a zero value on the boundary, resulting in

$$\phi_a = \tfrac{1}{2}\bar{\phi}_A. \tag{2.7}$$

The stencil of the transpose of this linear interpolation operator is (with scaling such that the sum of the weights is one in the interior)

$$[R]_i^{(-2)} = \tfrac{1}{32}\begin{bmatrix} 0 & 0 & 0 & 0 \\ 0 & 0 & 0 & 0 \\ 0 & 0 & e_i & e_i \\ 0 & 0 & e_i & e_i \end{bmatrix}, \quad [R]_i^{(-1)} = \tfrac{1}{32}\begin{bmatrix} 0 & 0 & 0 & 0 \\ 0 & 2 & 2 & 0 \\ 0 & 2 & 2+e_i & e_i \\ 0 & 0 & e_i & e_i \end{bmatrix},$$

$$[R]_i^{(0)} = \frac{1}{32}\begin{bmatrix} w_i & w_i & 0 & 0 \\ w_i & 2+w_i & 2 & 0 \\ 0 & 2 & 2 & 0 \\ 0 & 0 & 0 & 0 \end{bmatrix}, \quad [R]_i^{(1)} = \frac{1}{32}\begin{bmatrix} w_i & w_i & 0 & 0 \\ w_i & w_i & 0 & 0 \\ 0 & 0 & 0 & 0 \\ 0 & 0 & 0 & 0 \end{bmatrix}, \tag{2.8}$$

where w_i or e_i are zero if they refer to fine grid function values outside the domain; otherwise they are one.

It was found that all other partitions of the cube in tetrahedrons result in a restriction operator R such that, with P given by (2.5) and $\bar{A}$ by (2.3), $[\bar{A}]$ has more entries than [A] as given by (2.4).

3. COARSE GRID MATRICES

In this section we discuss the computer calculation of the sparsity pattern and the coarse grid matrix with (2.3). Let P given by (2.5) and R by (2.8). We may use the algorithm Structure given in [7] to determine the sparsity pattern $S_{\bar{A}}$ of $\bar{A}$. $S_{\bar{A}}$ is found to be the same as given by (2.4). For saving time and work we prefer the use of explicit expressions for the entries of $[\bar{A}]$ to their computation using the algorithm RAP [7]. The algebra involved becomes a bit too much to be carried out by hand. However, it is not difficult to write a computer program for the derivation of the desired formulas in three dimensions. A description of software and formulas obtained are given in [6]. Another advantage of using explicit formulas over direct computation of $\bar{A}$ is that these formulas can be efficiently implemented on vector and parallel computers in a straightforward way.

In the case $\sigma = 0$ in (1.1a) A and $\bar{A}$ take a particularly simple form with P given by (2.5) and R by (2.8). If

$$[A]_i^{(-1)} = \begin{bmatrix} 0 & 0 & 0 \\ 0 & w_{i-e_3} & 0 \\ 0 & 0 & 0 \end{bmatrix}, \quad [A]_i^{(0)} = \begin{bmatrix} 0 & v_i & 0 \\ u_{i-e_1} & s_i & u_i \\ 0 & v_{i-e_2} & 0 \end{bmatrix},$$

$$[A]_i^{(1)} = \begin{bmatrix} 0 & 0 & 0 \\ 0 & w_i & 0 \\ 0 & 0 & 0 \end{bmatrix}, \tag{3.1}$$

with $s_i = -(u_{i-e_1} + u_i + v_{i-e_2} + v_i + w_{i-e_3} + w_i)$, then $[\bar{A}] = [A]$ with overbars on u, v, w and s. We find

$$\bar{u}_i = (u_{2i-e_2-e_3} + u_{2i-e_3} + u_{2i-e_2} + u_{2i})/16 , \tag{3.2a}$$

$$\bar{v}_i = (v_{2i-e_1-e_3} + v_{2i-e_3} + v_{2i-e_1} + v_{2i})/16 , \tag{3.2b}$$

$$\bar{w}_i = (w_{2i-e_1-e_2} + w_{2i-e_2} + w_{2i-e_1} + w_{2i})/16 . \tag{3.2c}$$

Hence in this case $\bar{A}$ is symmetric and very cheap to obtain. The fact that in general $\bar{A}$ is not symmetric even if A is, because $P \neq R^T$, is not a serious disadvantage of the present method since the number of elements of $\bar{A}$ is only 1/8 of that of A.

4. SMOOTHING

In [3,5,8] several incomplete factorization iterative methods are analysed by local mode smoothing analysis and compared with respect to their smoothing behaviour in three–dimensional anisotropic diffusion problems. The only robust methods found (alternating plane relaxation) are complex and costly. Nevertheless satisfactory practical results are obtained with a not completely robust but simple smoothing based on modified incomplete point factorization (IPFM). This method is defined as follows. Let

$$A = P + T + L + d + U + S + Q \tag{4.1}$$

where the matrices P, T, L, d, U, S and Q correspond to the nonzero diagonal of A, d is the main diagonal (cf. Figure 4.1).

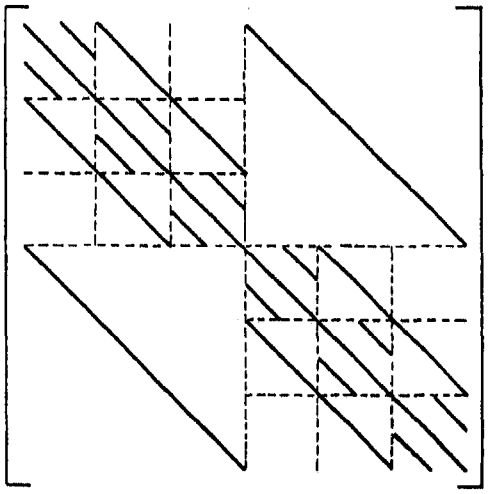

Figure 4.1. The diagonals P, T, L, d, U, S and Q of A from lower to upper respectively.

Let C be an approximation of A defined by:

$$C = (P + T + L + \delta)\delta^{-1}(\delta + U + S + Q)$$

with the element of δ at an internal node i defined by

$$\delta_i = d - L\delta_{i-e_1}^{-1}U - T\delta_{i-e_2}^{-1}S - P\delta_{i-e_3}^{-1}Q$$
$$- \omega[L\delta_{i-e_1}^{-1}(S+Q) + T\delta_{i-e_2}^{-1}(U+Q) + P\delta_{i-e_3}^{-1}(U+S)]$$

with $e_1 = (1,0,0)$, $e_2 = (0,1,0)$, $e_3 = (0,0,1)$ and ω a parameter that can be used to improve the smoothing factor. In the case of dominant direction (e.g. $D_1 \gg D_2 \approx D_3$) ω is taken –0.2 (cf. [8]); the related method is refered by IPFM(–0.2) (incomplete point factorization modified). In the case of dominant plane (e.g. $D_1 \approx D_2 \gg D_3$) good smoothing cannot be obtained with a single value of ω. After some empirical tests we found the smoother IPFM($\omega_1,\omega_2,\omega_3$), with $\omega_1 = -0.4$, $\omega_2 = 0.2$ and $\omega_3 = 0.75$, which consists of using IPFM(ω_i), $i = 1,2,3$, successively. IPFM(–0.2) will be used for isotropic or dominant direction problems and IPFM($\omega_1,\omega_2,\omega_3$) otherwise.

5. NUMERICAL EXPERIMENTS

To investigate the efficiency of the cell–centered multigrid method three test problems will be used. These test problems concern anisotropy and interface discontinuities of the coefficients. Boundary conditions are taken such that the matrices are definite. Almost singular problems are not studied here. All problems are of the type (1.1a,b) and solved in cube with N cells in x_1–, x_2– and x_3–direction. The interfaces are planes of the mesh, so that harmonic averaging for the diffusion coefficients is used.

5.1 Test problems

Problem 1 [1]: Anisotropic coefficients.

The domain Ω is [0,1] × [0,1] × [0,1]. The diffusion coefficients are as follows: $D_1 = 1$, $D_2 = 10^3$, $D_3 = 10^{-3}$. The right–hand side is

$$f(x_1,x_2,x_3) = \begin{cases} 1\ , & (x_1,x_2,x_3) = (h/2,h/2,h/2)\ ,\ \ h = 1/N \\ \\ 0\ , & \text{otherwise} \end{cases}$$

and σ is zero.

The following Dirichlet boundary condition is prescribed:

$$\varphi|_{\partial\Omega} = x_1^2 + x_2^2 + x_3^2.$$

For problems 2 and 3 we define the following partition of the cube Ω in eight cubes Ω_i, $i = 1,\ldots,8$.

Let $\Omega = [0,L] \times [0,L] \times [0,L]$. $\bar{L}$ designates the position of the interfaces. We define:

$$\Omega_1 = \{(x_1,x_2,x_3): 0 \le x_1 < \bar{L}\,,\ 0 \le x_2 < \bar{L}\,,\ 0 \le x_3 < \bar{L}\}$$

$$\Omega_2 = \{(x_1,x_2,x_3): \bar{L} \le x_1 \le L\,,\ 0 \le x_2 < \bar{L}\,,\ 0 \le x_3 < \bar{L}\}$$

$$\Omega_3 = \{(x_1,x_2,x_3): 0 \le x_1 < \bar{L}\,,\ \bar{L} \le x_2 \le L\,,\ 0 \le x_3 < \bar{L}\}$$

$$\Omega_4 = \{(x_1,x_2,x_3): \bar{L} \le x_1 < L\,,\ \bar{L} \le x_2 \le L\,,\ 0 \le x_3 < \bar{L}\}$$

$$\Omega_5 = \{(x_1,x_2,x_3): 0 \le x_1 < \bar{L}\,,\ 0 \le x_2 < \bar{L}\,,\ \bar{L} \le x_3 \le L\}$$

$$\Omega_6 = \{(x_1,x_2,x_3): \bar{L} \le x_1 \le L\,,\ 0 \le x_2 < \bar{L}\,,\ \bar{L} \le x_3 \le L\}$$

$$\Omega_7 = \{(x_1,x_2,x_3): 0 \le x_1 < \bar{L}\,,\ \bar{L} \le x_2 \le L\,,\ \bar{L} \le x_3 \le L\}$$

$$\Omega_8 = \{(x_1,x_2,x_3): \bar{L} \le x_1 \le L\,,\ \bar{L} \le x_2 \le L\,,\ \bar{L} \le x_3 \le L\}$$

Problem 2 [2]: Discontinuous coefficients.

The domain Ω is $[0,N] \times [0,N] \times [0,N]$ ($h = 1$). The diffusion coefficients D_α are such that $D_1=D_2=D_3=D$ with

$$\begin{cases} D = 10^3 & \text{in } \Omega_i\,,\ i = 1,4,6,7 \\ D = 1 & \text{in } \Omega_i\,,\ i = 2,3,5,8\,. \end{cases}$$

The right–hand side is defined by

$$\begin{cases} f = 0 & \text{in } \Omega_i\,,\ i = 1,4,6,7 \\ f = 1 & \text{in } \Omega_i\,,\ i = 2,3,5,8 \end{cases}$$

and $\sigma = \dfrac{1}{3D}$.

The following boundary conditions are prescribed

$$\begin{cases} \varphi(x_1,x_2,x_3) = x_1^2 + x_2^2 + x_3^2 & \text{on } x_1 = 0,N\,,\ x_2 = 0,N \\ \dfrac{\partial\varphi}{\partial n} + \dfrac{1}{2D}\varphi = 0 & \text{on } x_3 = 0,N. \end{cases}$$

Problem 3 [1,2]: Anisotropic discontinuous coefficients.

The domain Ω is [0,1] × [0,1] × [0,1]. The diffusion coefficients are such that:

$$D_1 = \begin{cases} = 1 & \text{in } \Omega_i\,,\ i = 1,3,5,7 \\ \\ = 10^{-2} & \text{in } \Omega_i\,,\ i = 2,4,6,8 \end{cases}$$

$$D_2 = \begin{cases} = 10^{2} & \text{in } \Omega_i\,,\ i = 1,2,5,6 \\ \\ = 1 & \text{in } \Omega_i\,,\ i = 3,4,7,8 \end{cases}$$

and

$$D_3 = \begin{cases} = 10^{-2} & \text{in } \Omega_i\,,\ i = 1,2,3,4 \\ \\ = 10^{2} & \text{in } \Omega_i\,,\ i = 5,6,7,8\,. \end{cases}$$

The right–hand side and boundary conditions are those given for problem 1, σ is zero.

For the tests performed here we used the W–cycle. The smoother used is IPFM(–0.2) or IPFM(–0.4,0.2,0.75). One postsmoothing is done. On the coarsest grid the solution is obtained using the QR method. The initial iterand is zero. The following reduction factor:

$$\kappa = \frac{\|r^{(m)}\|_2}{\|r^{(m-1)}\|_2} \tag{5.1}$$

and the average reduction factor

$$\bar{\kappa} = \sqrt[m]{\frac{\|r^{(m)}\|_2}{\|r^{(0)}\|_2}}\,, \tag{5.2}$$

where $r^{(m)}$ is the residual at iteration number m, are reported for $m = 15$. In some cases CPU times are given. The computations are done on CONVEX C210. No special effort was done to make the algorithm suitable for vectorization.

5.2 Numerical results

Table 1 presents the results of cell–centered multigrid (MGCC) for problem 1 using the smoothers IPFM(–0.2) and IPFM(–0.4,0.2,0.75). The results are in accordance with smoothing analysis results [8] which predicts efficiency.

	(a)		(b)	
h	κ	$\bar{\kappa}$	κ	$\bar{\kappa}$
1/16	0.049	0.032	9.10^{-5}	5.10^{-5}
1/24	0.110	0.066	0.001	6.10^{-4}
1/32	0.184	0.105	0.005	0.003

Table 1. κ and $\bar{\kappa}$ for problem 1:
(a) MGCC with IPFM(–0.2)
(b) MGCC with IPFM(–0.4,0.2,0.75)

Table 2a gives results for problem 2 with interfaces common to all or almost all grids.

		(a)		(b)	
N	$\bar{L}$	κ	$\bar{\kappa}$	κ	$\bar{\kappa}$
16	8	0.371	0.248	0.145	0.090
24	12	0.498	0.342	0.189	0.102
32	16	0.447	0.276	0.215	0.124
48	24	0.536	0.341	0.252	0.136

Table 2a. κ, $\bar{\kappa}$ for problem 2
(a) MGCC with IPFM(–0.2)
(b) MGCC with IPFM(–0.4,0.2,0.75)

MGCC with IPFM(–0.2) or IPFM(–0.4,0.2,0.75) performs very well in this case. A weak dependence of the rate of convergence on h is noticeable.

Table 2b gives results for problem 2 when interfaces are present only on the finest grid. The rate of convergence is worse than in the previous case but is still acceptable. IPFM(–0.4,0.2,0.75) has better smoothing properties but is less efficient than IPFM(–0.2) because of its higher cost. Column (c) of Table 2b gives results with MGCC (smoothing: IPFM(–0.2)) accelerated by Orthomin [13] with only two orthogonalizations. We see that acceleration with Orthomin helps to improve considerably robustness and efficiency of MGCC. It is found that the residual reduction with (a) after 15 iterations is obtained already with (c) after 7 or fewer iterations. We do not report κ when Orthomin is applied because this quantity behaves erratically.

		(a)		(b)		(c)
N	$\bar{L}$	κ	$\bar{\kappa}$	κ	$\bar{\kappa}$	$\bar{\kappa}$
16	9	0.665	0.499	0.350	0.264	0.240
24	13	0.727	0.533	0.447	0.324	0.272
32	17	0.737	0.527	0.498	0.352	0.292
48	25	0.781	0.546	0.560	0.384	0.314

Table 2b. κ, $\bar{\kappa}$ for problem 2
(a) MGCC with IPFM(–0.2)
(b) MGCC with IPFM(–0.4,0.2,0.75)
(c) MGCC with IPFM(–0.2) and acceleration by Orthomin, number of orthogonalization (nbort) = 2.

Tables 3a, 3b, 3c and 3d give the results of MGCC using IPFM(–0.2) or IPFM(–0.4,0.2,0.75) with and without Orthomin acceleration for problem 3. The interfaces are common to all or almost all grid (case 1) in Tables 3a, 3c and are present on only the finest grid (case 2) in Tables 3b, 3d.

		(a)		(b)
h	$\bar{L}$	κ	$\bar{\kappa}$	$\bar{\kappa}$
1/16	0.5	0.870	0.561	0.570
1/24	0.5	0.923	0.569	0.434
1/32	0.5	0.928	0.567	0.476
1/48	0.5	0.933	0.561	0.505

Table 3a. κ, $\bar{\kappa}$ for problem 3, case 1.
(a) MGCC with IPFM(–0.2)
(b) MGCC with IPFM(–0.2) and Orthomin, nbort = 2.

		(a)		(b)
h	$\bar{L}$	κ	$\bar{\kappa}$	$\bar{\kappa}$
1/16	0.5625	0.863	0.559	0.361
1/24	0.5417	0.916	0.571	0.439
1/32	0.5313	0.926	0.569	0.482
1/48	0.5208	0.928	0.564	0.505

Table 3b. κ, $\bar{\kappa}$ for problem 3, case 2.
(a) MGCC with IPFM(–0.2)
(b) MGCC with IPFM(–0.2) and Orthomin, nbort = 2.

		(a)			(b)	
h	$\bar{L}$	κ	$\bar{\kappa}$	CPU (sec)	$\bar{\kappa}$	CPU (sec)
1/16	0.5	0.446	0.290	9	0.100	10
1/24	0.5	0.704	0.423	28	0.200	29
1/32	0.5	0.822	0.470	68	0.278	71
1/48	0.5	0.911	0.490	213	0.348	216

Table 3c. κ, $\bar{\kappa}$ and CPU time (seconds) for problem 3, case 1.
(a) MGCC with IPFM(–0.4,0.2,0.75)
(b) MGCC with IPFM(–0.4,0.2,0.75) and Orthomin, nbort = 2.

		(a)		(b)
h	$\bar{L}$	κ	$\bar{\kappa}$	$\bar{\kappa}$
1/16	0.5625	0.434	0.282	0.097
1/24	0.5417	0.700	0.421	0.359
1/32	0.5313	0.820	0.469	0.345
1/48	0.5208	0.910	0.490	0.374

Table 3d. κ, $\bar{\kappa}$ for problem 3, case 2.
(a) MGCC with IPFM(–0.4,0.2,0.75)
(b) MGCC with IPFM(–0.4,0.2,0.75) and Orthomin, nbort = 2.

IPFM(–0.2) is not a good smoother for this problem with dominant plane anisotropy as predicted by smoothing analysis [8]. The bad performance of MGCC for problem 3 when

h becomes small (cf. Tables 3c, (a), 3d, (a)) is due essentially to the non–robustness of the smoother IPFM(–0.4,0.2,0.75). Acceleration of MGCC by Orthomin (using two orthogonalization only) improves efficiently its convergence (cf. column (b) of Tables 3a, 3b, 3c and 3d) for IPFM(–0.4,0.2,0.75) and IPFM(–0.2) smoother. This acceleration does not increase significantly the CPU time (cf. Table 3c). The convergence depends weakly on h, as in the previous test problems. This is due to the fact that the smoothing behaviour depends on h.

These numerical experiments show that cell–centered multigrid can handle three–dimensional interface problems and anisotropic problems when a suitable smoother is used. Acceleration with Orthomin improves considerably the convergence of MGCC when the smoother is weak.

6. STORAGE AND PRELIMINARY WORK

In this section we compare storage and preliminary work for vertex–centered [1,2,3,9,10] and cell–centered multigrid for interface problems. On the finest grid for both methods, we have to store the matrix of the system, its right–hand side and the solution. Assuming for A a 7–point stencil, this requires $10n$ words, n being the number of finest grid cells. On coarse grids, cell–centered multigrid requires $17n\,[\frac{1}{8} + \frac{1}{64} + \ldots] < \frac{17}{7}\,n$ words for the storage of restriction of residuals, corrections and the matrices $A_k = RA_{k-1}P$, $k = 2,\ldots,\ell$ with ℓ the number of the grids used while vertex–centered multigrid requires $29n\,[\frac{1}{8} + \frac{1}{64} + \ldots] < \frac{29}{7}\,n$ words. Vertex–centered multigrid needs $26n\,[\frac{1}{8} + \frac{1}{64} + \ldots] < \frac{26}{7}\,n$ words for the storage of matrix–dependent transfer operators. This is summarized in Table 4 for comparison.

The preliminary work involves for both methods the calculation of A_k and the smoothing set–up (factorization). Vertex–centered multigrid requires in addition the calculation of the matrix–dependent transfer operator. Explicit expressions for A_k, $k = 2,\ldots,\ell$ seem out of reach in vertex–centered case. Using stencil notation ([7]) a simple well–structured algorithm to compute A_k is easily designed. Explicit expressions

of the elements of A_k are easy to obtain in the cell–centered case [6]. The work involved for the calculation of A_k, $k = 2,...,\ell$ in the cell–centered case when explicit expressions are used and in the vertex–centered case when A_k is computed directly are given in Table 4.

(a)				(b)	
v.c.		c.c.		v.c.	c.c.
+	*	+	*	$\frac{125}{7}$ n	$\frac{87}{7}$ n
1701	3456	315	45		

Table 4. (a) computing work per coarse grid point for $\bar{A}_k$, $k = 2,...,\ell$ for vertex–centered multigrid (v.c.) and cell–centered multigrid (c.c.)
(b) storage for v.c. and c.c.
+: addition and subtraction; *: multiplication and division

It is clear that cell–centered requires significantly less storage (70%) and preliminary work than vertex–centered multigrid. Furthermore, it is obvious that other operations, such as incomplete factorization, smoothing, matrix–vector multiplication, etc., are less costly with 15–point coarse grid stencils (cell–centered) than with 27–point coarse grid stencils (vertex–centered).

7. CONCLUDING REMARKS

An extension of cell–centered multigrid (MGCC) to three dimensions has been given. Transfer operators and coarse grid Galerkin approximation are discussed. Furthermore, numerical results for some three–dimensional problems with discontinuous and anisotropic coefficients are presented. Using IPFM(–0.2) or IPFM(–0.4,0.2,0.75) as smoother, MGCC is efficient for interface or anisotropic problems for which the smoothing analysis predicts efficient reduction of short wavelengths of the error. Dependence of the convergence rate of MGCC on the location of interfaces and on the fine grid mesh–size is noticed but is acceptable in all cases. Acceleration of MGCC by a Lanczos type method, namely Orthomin, improves significantly its convergence rate, so

that in all cases an efficient method results.

For interface problems, vertex–centered multigrid requires matrix–dependent transfer operators, which makes the method more complicated and costly per iteration than cell–centered multigrid. We have not implemented vertex–centered multigrid in three dimensions, so rates of convergence are not compared directly. See [1,2,10] for numerical experiments with vertex–centered multigrid in three dimensions.

REFERENCES

[1] Behie, A. and Forsyth, P.A.: Multigrid solution of three–dimensional problems with discontinuous coefficients. Appl. Math. Comput. **13** (1983), 673–685.

[2] Dendy, J.E., Jr.: Two multigrid methods for three–dimensional problems with discontinuous and anisotropic coefficients. SIAM J. Sci. Stat. Comp. **8** (1987), 673–685.

[3] Kettler, R.: Linear multigrid method for numerical reservoir simulation. Ph.D. Thesis, University of Technology, Dept. of Technical Mathematics and Informatics, Delft, December 1987.

[4] Kettler, R.: Analysis and comparison of relaxation schemes in robust multigrid and preconditional conjugate methods. In: W. Hackbusch and U. Trottenberg (eds.), Multigrid methods. Proceedings, Köln–Porz, 1981. Lect. Notes in Math. 960, 502–534, Springer–Verlag, Berlin 1982.

[5] Kettler, R. and Wesseling, P.: Aspects of multigrid methods for problems in three dimensions. Aplied Math. Comp. **19** (1986), 159–168.

[6] Khalil, M., Van Kan, J.J.I.M. and Wesseling, P.: Prolongation, restriction and coarse grid approximation in a three–dimensional cell–centered multigrid method. Report 88–02, University of Technology, Dept. of Technical Mathematics and Informatics, Delft, 1988.

[7] Khalil, M. and Wesseling, P.: Vertex–centered and cell–centered multigrid methods for interface problems. Report 88–42, Dept. of Technical Mathematics and Informatics, Delft University of Technology, 1988.

[8] Khalil, M.: Local mode smoothing analysis for various incomplete factorization iterative methods in three dimensions. To appear as report of Dept. of Technical Mathematics and Informatics, Delft University of Technology, 1989.

[9] Puiseux, P.: Méthode Multigrille pour la résolution de modèles mathématiques de l'industrie pétrolière. Thèse de Doctorat de l'Université de Pau, Juillet 1988.

[10] Scott, T.: Multigrid methods for oil reservoir simulation in three dimensions. In: Paddon, D.J. and Holstein, H. (eds.), Multigrid methods for integral and differential equations. The Institute of Mathematics and its Applications Conference Series, New Series Number 3, Clarendon Press, Oxford 1985, 283–300.

[11] Sonneveld, P., Wesseling, P. and De Zeeuw, P.M.: Multigrid and conjugate gradient methods as convergence acceleration techniques. In: Paddon, D.J. and Holstein, H. (eds.), Multigrid methods for integral and differential equations. The Institute of Mathematics and its Applications Conference Series, New Series Number 3, Clarendon Press, Oxford 1985, 117–167.

[12] Thole, C.A. and Trottenberg, U.: Basic smoothing procedures for the multigrid treatment of elliptic 3–D operators. Applied Math. Comp. 19 (1986), 333–345.

[13] Vinsome, P.W.: Orthomin, an iterative method for solving sparse sets of simultaneous linear equation. In: Proceedings of the 4th SPE Symposium of Reservoir Performance, 1976, 149–159, Society of Petroleum Engineers of AIME, Paper SPE 5729.

[14] Wesseling, P.: Cell–centered multigrid for interface problems. J. Comput. Phys. 79 (1988), 85–91.

APPENDIX

A.1. Discretization

We consider the problem (1.1) with D_α, σ and f discontinuous across internal interfaces. The domain Ω is uniformly subdivided in cells. The interfaces consist of faces of cells. The unknowns φ_i are located at the centers $((i_1-\frac{1}{2})h_1, (i_2-\frac{1}{2})h_2, (i_3-\frac{1}{2})h_3)$ of the cells Ω_i, $i \equiv (i_1,i_2,i_3)$, $1 \le i_\alpha \le N_\alpha$, N_α being the number of cells in the direction x_α.

Integrating (1.1a) over $V = \Omega_i$ we obtain

$$-\int_{\partial V} \sum_{\alpha=1}^{3} D_\alpha \frac{\partial \varphi}{\partial x_\alpha} n_\alpha \, ds + \int_V \sigma\varphi \, dV = \int_V f \, dV \tag{A.1}$$

with n_α the component in the direction x_α of the normal to the boundary directed away from the interior of V.

Let V given by Figure A.1.

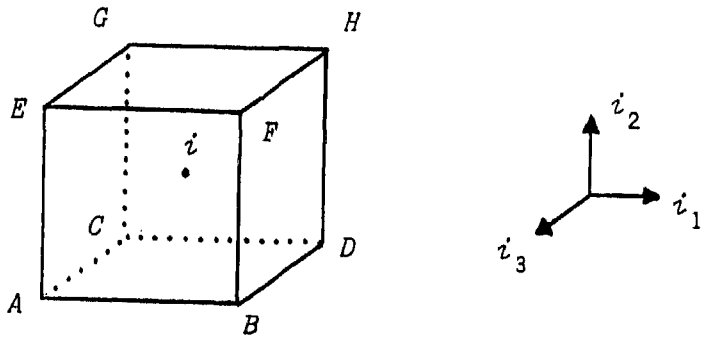

Figure A.1. Cell $V \equiv \Omega_i$

We define the faces $S_1 = ACGE$, $S_2 = BDHF$, $S_3 = ABCD$, $S_4 = EFGH$, $S_5 = CDGH$ and $S_6 = ABEF$.

A.2. Stencil at the interior cells

We have for surface integrals in (A.1),

$$\int_{S_1} D_1 \frac{\partial \varphi}{\partial x_1} \, dx_2 \, dx_3 \approx \frac{h_2 h_3}{h_1} W^1_{i-e_1} (\varphi_i - \varphi_{i-e_1}) \tag{A.2}$$

with

$$W^1_{i-e_1} = 2 \frac{D_{1,i} \cdot D_{1,i-e_1}}{D_{1,i} + D_{1,i-e_1}} \tag{A.3}$$

where $e_1 = (1,0,0)$. The integrals over S_β, $\beta = 2,\ldots,6$ are handled similarly.

The second term in (A.1) can be approximated by

$$\int_V \sigma\varphi \, dV \approx h_1 h_2 h_3 \sigma_i \,. \tag{A.4}$$

The stencil of the matrix at a center i of an interior cell is then given by

$$[A]_i^{(-1)} = \begin{bmatrix} 0 & & \\ 0 & -s_3 W^3_{i-e_3} & 0 \\ & 0 & \end{bmatrix}, \quad [A]_i^{(0)} = \begin{bmatrix} & -s_2 W^2_i & \\ -s_1 W^1_{i-e_1} & \text{sum} + h_1 h_2 h_3 \sigma_i & -s_1 W^1_i \\ & -s_2 W^2_{i-e_2} & \end{bmatrix},$$

$$[A]_i^{(1)} = \begin{bmatrix} 0 & & \\ 0 & -s_3 W^3_i & 0 \\ & 0 & \end{bmatrix}, \tag{A.5}$$

with

$$\text{sum} = s_1(W^1_{i-e_1} + W^1_i) + s_2(W^2_{i-e_2} + W^2_i) + s_3(W^3_{i-e_3} + W^3_i) \tag{A.6}$$

where $s_\gamma = \dfrac{h_\alpha h_\beta}{h_\gamma}$, $\alpha,\beta,\gamma \in \{1,2,3\}$, $\alpha \neq \beta \neq \gamma$ and $e_2 = (0,1,0)$, $e_3 = (0,0,1)$. W^2_i and W^3_i are defined as W^1_i (A.3).

A.3. Stencil at boundary cells

A.3.1 Dirichlet boundary condition

Let $b = 0$ and $c = 1$ in (1.1b). We have

$$\varphi\big|_{\partial\Omega} = g. \tag{A.7}$$

Let V be a cell with only the face S_1 on $\partial\Omega$. Let M be the center of S_1. We have

$$\int_{S_1} D_1 \frac{\partial\varphi}{\partial x_1} \, dx_2 \, dx_3 = 2 \, s_1 D_{1,i}(\varphi_i - \varphi_M). \tag{A.8}$$

As $\varphi_M = g_M$ is known, we obtain the following stencil

$$[A]_i^{(0)} = \begin{bmatrix} & -s_2 W^2_i & \\ 0 & \text{sum} + 2s_1 D_{1,i} + h_1 h_2 h_3 \sigma_i & -s_1 W^1_i \\ & -s_2 W^2_{i-e_2} & \end{bmatrix} \tag{A.9}$$

with $[A]_i^{(\pm 1)}$ the same as in (A.5) and

$$\text{sum} = s_1 W^1_i + s_2(W^2_{i-e_2} + W^2_i) + s_3(W^3_{i-e_3} + W^3_i) \,. \tag{A.10}$$

The cases when V is a cell with another face than S_1 or more than one face on $\partial\Omega$ are easily deduced from the previous one.

A.3.2 Neumann or Robbins boundary condition

Let $b = 1$ in (1.1b), i.e.:

$$\frac{\partial\varphi}{\partial n} + c\varphi = g\,, \quad c \geq 0. \tag{A.11}$$

Let V be a cell with only the face S_1 on $\partial\Omega$. Let M be the center of S_1 and P the center of V. The following approximation is made:

$$\left[\frac{\partial\varphi}{\partial n}\right]_M \approx \frac{2(\varphi_M - \varphi_P)}{h_1} \tag{A.12}$$

or

$$\varphi_M - \varphi_P \approx \tfrac{1}{2} h_1 (g - c\varphi)_M\,. \tag{A.13}$$

Hence

$$\varphi_M = (\tfrac{1}{2} h_1 g_M - \varphi_P)/(1 + \tfrac{1}{2} h_1 c_M)\,. \tag{A.14}$$

The surface integral on S_1 is then

$$\int_{S_1} D_1 \frac{\partial\varphi}{\partial x_1}\,dx_2\,dx_3 \approx h_2 h_3 D_{1,i} \frac{\partial\varphi}{\partial x_1}\bigg|_M \approx -h_2 h_3 D_{1,i}(g_M - c_M\varphi_M). \tag{A.15}$$

By substitution of φ_M given by (A.14) one obtains

$$\int_{S_1} D_1 \frac{\partial\varphi}{\partial x_1}\,dx_2\,dx_3 \approx \frac{2\,h_2 h_3}{2 + h_1 c_M} D_{1,i}(c_M\varphi_i - g_M)\,. \tag{A.16}$$

The stencil at P is then

$$[A]_i^{(0)} = \begin{bmatrix} & -s_2 W_i^2 & \\ 0 \quad \text{sum} + \dfrac{2h_2 h_3 c_M}{2 + h_1 c_M} D_{1,i} + h_1 h_2 h_3 \sigma_i & & -s_1 W_i^1 \\ & -s_2 W_{i-e_2}^2 & \end{bmatrix}, \tag{A.17}$$

with sum given by (A.10) and $[A]_i^{(\pm 1)}$ as in (A.5).

The other cases where V is adjacent to $\partial\Omega$ are deduced from the previous case.

The following reports have appeared in this series:

89-25	Roelof Koekoek	Generalizations of Laguerre polynomials
89-26	Jan van Mill and Petr Simon	A point in $\beta Z \setminus Z$ not contained in a maximal orbit closure
89-27	S. Zeng and P. Wesseling	A multigrid method combined with defect correction for free convection problems at high Rayleigh numbers
89-28	Maria Polkowska-Semeniuk Lech T. Polkowski	Some techniques for anaphora resolution in algebraic linguistics
89-29	A.J. van Zanten	Binary Gray codes and index systems
89-30	D.H.J. Epema	An expert system for VM performance analysis
89-31	Ph. Clément and P. Egbetrs	On the sum of two maximal monotone operators
89-32	J.A.C. Resing, G. Hooghiemstra, M.S. Keane	The M/G/1 processor sharing queue as the almost sure limit of feedback queues
89-33	I.E. van de Water en P.A.H.M. Mantelaers	Referentiekader documentaire informatievoorziening
89-34	A.J. Hermans, E. van Sabben, J.A. Pinkster	A device to extract energy from water waves
89-35	M. Khalil and P. Wesseling	A cell-centered multigrid method for three-dimensional anisotropic-diffusion and interface problems

Copies of these reports may be obtained from the bureau of the Faculty of Technical Mathematics and Informatics, Julianalaan 132, 2628 BL DELFT, phone 015-784568.